Pulse timing jitter estimated from optical phase noise in mode-locked semiconductor quantum dash lasers

Mao, Youxin; Lu, Zhenguo; Liu, Jiaren; Poole, Philip J.; Liu, Guocheng

Publisher's version / Version de l'éditeur:
https://doi.org/10.1109/JLT.2020.2996424
Journal of Lightwave Technology, 38, 17, pp. 4787-4793, 2020-05-21

Pulse Timing Jitter Estimated From Optical Phase Noise in Mode-Locked Semiconductor Quantum Dash Lasers

Youxin Mao, Zhenguo Lu, Jiaren Liu, Philip J. Poole, and Guocheng Liu

Abstract—**The determination of timing jitter obtained from optical phase noise measurements is investigated in InAs/InP quantum dash Fabry–Pérot mode-locked coherent comb lasers with different pulse repetition rates. The results are compared with those determined through a direct measurement of the first harmonic of the RF power spectrum. Very good agreement is achieved. The ability to measure the timing jitter from optical phase noise is not restricted by the repetition rate of the laser being studied, allowing it to be applied to extremely high repetition rate lasers. Using these lasers we demonstrate 5.4 Tbit/s (PAM-4 48 $\times$ 28 GBaud PDM) and 10.3 Tbit/s (16 QAM 56 $\times$ 23 GBaud PDM) aggregate data transmission capacity. The ultra-low timing jitter exhibited by these devices make them excellent sources for multi-terabit optical networks.**

Index Terms—**Mode-lock lasers, Phase noise, Quantum dot devices, Semiconductor laser, Timing jitter.**

I. Introduction

SEMICONDUCTOR-BASED monolithic coherent comb lasers (CCLs) with their ability to emit stable optical pulse trains at high repetition rate and narrow pulse widths are a promising technology for optical communications [1]. Other advantages include compact size, low power consumption, simple fabrication, and the ability for hybrid integration with silicon substrates. CCLs utilizing quantum dots or dashes (QD) rather than quantum wells are particularly attractive due to the reduced amount of amplified spontaneous emission leading to lower intrinsic noise, narrower linewidth, and hence ultra-low timing jitter. They are promising sources for the next generation of high speed optical networks, optical signal processing and millimeter wave generation [2]. For all these applications, low timing jitter is necessary in order to fulfill low bit error rate and high sampling accuracy. While the mode-locking mechanism for these single section QD lasers is not fully understood, recent theoretical studies [3] suggest that the enhanced spatial hole burning in QD vs. QW devices due to a reduced lateral carrier diffusion is very important. This in combination with non-linear phase sensitive effects, such as four wave mixing (FWM) in the gain medium, lead to self-locking of beat frequencies among the lasing modes [3], [4], i.e., passively mode-locking (PML). With the high modal gain available in the QD based active layers [5] and no extra cavity losses introduced by a saturable absorber section, the cavity length in these devices can be made short enough to achieve extremely high repetition rates, with reported values of up to 346 GHz [6]. Due to the inherent simplicity of implementation of these single section QD lasers as compared to other techniques such as hybrid or actively mode-locking (AML) they are very interesting to study, and the evaluation of their timing jitter behavior becomes particularly important [7].

A commonly used timing jitter estimation method was developed by von der Linde [8]. This method is based on the assumption that timing fluctuations are stationary stochastic processes, and measurement of the power spectral density (PSD) from photodiode signals can be used to calculate the root-mean-squared (rms) timing jitter, which is valid only for AML lasers [9]. For PML lasers, the variance of the timing fluctuations increases with time and exhibits a Gaussian random walk behavior, indicating a non-stationary stochastic process [9]. To overcome the drawback of the von der Linde method, an optical technique for pulse-to-pulse timing jitter using optical cross correlation has been used [10]. However, the high measurement error when the time jitter is smaller than the autocorrelation width, and the high power levels required for second harmonic generation in the nonlinear crystal limit its applicability [10]. A pulse-to-pulse time jitter estimation method was proposed specifically for a PML laser in [11]. The properties of intrinsic phase noise from relatively broadband spontaneous emission in the PML laser leads to a Lorentzian shaped PSD of photocurrent RF phase noise. Studying linewidth of the first harmonic of photocurrent RF can provide a simple and appropriate way to characterize the timing jitter of the PML lasers. This method overcomes the limits of measuring the time jitter by optical cross correlation which requires high pulse peak power. However, to measure the RF PSD requires the use of a photodetector that can respond at a frequency corresponding to the repetition rate of the laser pulse train. Due to the bandwidth limitation of available photodiodes, this restricts the application of this technique to repetition frequencies below 100 GHz. A technique for measuring timing jitter, using the optical spectrum of the longitudinal lasing modes of the PML laser, has been recently studied [12]–[14].

Manuscript received February 19, 2020; revised May 1, 2020; accepted May 11, 2020. Date of publication May 21, 2020; date of current version September 1, 2020. This work was supported by National Research Council Canada's high throughput and secure networks (HTSN) research program. *(Corresponding author: Youxin Mao.)*

The authors are with the Advanced Electronics and Photonics Research Center, National Research Council Canada, Ottawa K1A 0R6, Canada (e-mail: youxin.mao@nrc-cnrc.gc.ca; zhenguo.lu@nrc-cnrc.gc.ca; jiaren.liu@nrc-cnrc.gc.ca; philip.poole@nrc-cnrc.gc.ca; guocheng.liu@nrc-cnrc.gc.ca).

Color versions of one or more of the figures in this article are available online at https://ieeexplore.ieee.org.

Digital Object Identifier 10.1109/JLT.2020.2996424

Ref. [12] points out that the linewidth of longitudinal modes in a PML is determined mainly by two mechanisms: (1) the phase noise induced by the amplitude noise originated from the spontaneous emission noise, and (2) the phase noise induced by the random walk timing jitter. This results in the linewidth of longitudinal modes being a parabolic function of the mode number (wavelength) and reaches a minimum within the lasing spectrum. In [13], an explicit expression is deduced relating the optical linewidth to the mode number and the scaling of the parabola is proportional to the first harmonic of the RF linewidth, therefore it provides a direct measurement of the timing jitter. It is in agreement with their experimental investigations on a two-section hybrid mode-locked laser emitting at 1.3 μm [13]. A simple general formula is proposed [14] relating the pulse-to-pulse timing jitter diffusion constant to the optical mode linewidths of a semiconductor laser in the PML regime, and the present experimental results help validate this relationship in single-section QD ML lasers. This timing jitter measurement based on the optical spectrum is simple and not restricted by the repetition rate of the laser being measured.

We have previously demonstrated InAs/InP QD CCLs with pulse repetition rates from 10 GHz to 437 GHz and a total output power up to 50 mW per facet at room temperature [15]–[17]. We have recently demonstrated femtosecond timing jitter in an external cavity self-injection feedback locked InAs/InP QD 25 GHz C-band CCL by analysis of the Lorentzian linewidth of the first harmonic RF PSD [18]. In this paper we report a timing jitter study of single-section PML lasers with 11, 25, and 34.5 GHz pulse repetition frequencies by a parabolic fit of the optical linewidth obtained from optical phase noise measurements as a function of the optical longitudinal lasing modes. A comparison is made of the timing jitter measured from the optical phase noise and from directly measuring the RF PSD. Very good agreement is achieved. Finally we report on the application of these lasers for Terabit/s optical communication links.

II. Theory

The general noise influences in a mode-locked semiconductor lasers are mainly from the amplitude, the central optical frequency, the pulse frequency spacing, the pulse-to-pulse timing, and the optical phase, but the broadening of the comb lineshape is dominated by the contributions of optical phase noise and pulse-to-pulse timing fluctuations for the PML CCL [12], [13]. The phase and timing fluctuations in each mode are affected by amplified spontaneous emission noise going through a random walk process [13], [19]. Therefore, the timing jitter exhibits a diffusion-like behavior. If $\Delta t_r(t)$ expresses the timing fluctuations in the mode position at time *t*, the timing jitter σ can be described by a Gaussian random process with mean = 0 and total variance $\sigma = \langle|\Delta t_r(t)|^2\rangle = Dt$, where *D* is the timing jitter diffusion constant. Then phase fluctuation follows the behavior $\Delta\theta(t) = 2\pi\upsilon_r\Delta t_r(t)$. From analyzing the complex electric field of a semiconductor PML laser, considering only the effects of phase and timing fluctuations, the complex optical field is [13]

$$\mathrm{E}(\mathrm{t}) = \sum_{n=-\infty}^{\infty} A\left[t - nT_r - \Delta t(n)\right] e^{-j[2\pi\upsilon_r(t-nT_r)+\Delta\theta(n)+\phi(n)]} \tag{1}$$

where A(n), Δt(n), υ_{r}(n), $\Delta\theta$(n), and ϕ(n) are respectively the mode envelope, timing fluctuations, the center frequency, phase noise, and static phase of the nth longitudinal mode. T_r is the repetition period. Following [20], the optical spectrum can be calculated by taking the electric field autocorrelation function and Fourier transform. A set of Lorentzian modes with frequencies υ_{n} and the full-width at half-maximum (FWHM) linewidths $\Delta\upsilon_n$ compose the optical spectrum as

$$\mathrm{S}(\upsilon) \sim \frac{\left|\hat{A}(\upsilon - \upsilon_r)\right|^2}{\pi} \sum_{n=-\infty}^{\infty} \frac{\Delta\upsilon_n}{(\upsilon - \upsilon_n)^2 + \Delta\upsilon_n{}^2} \tag{2}$$

where $\hat{A}$ is the Fourier transform of the mode envelope. The quantum limited optical phase noise and timing jitter random walk fluctuations induce the Lorentzian mode shape in all the comb modes [13]. The FWHM optical mode linewidth is [14]

$$\Delta\upsilon_n = \Delta\upsilon_{\min} + 2\pi\upsilon_r^2 D(n - n_{\min})^2 \tag{3}$$

where $\mathrm{n}_{\min}$ is the mode number corresponding to the minimum linewidth $\Delta\upsilon_{\min}$, $\upsilon_r = 1/T_r$ is the repetition rate. In the same way, the spectrum of the laser intensity, or more commonly called the RF spectrum, can be calculated as a set of Lorentzians with the FWHM linewidth of *m*th harmonic expressed by $\Delta\nu_{RFm}$ [13]

$$S_{RF}(\upsilon) \sim \frac{1}{\pi} \sum_{n=-\infty}^{\infty} \frac{\Delta\upsilon_{RFm}}{(\upsilon - \mathrm{m}\upsilon_r)^2 + \Delta\upsilon_{RFm}^2} \tag{4}$$

It is found to consist of a sum of Lorentzian modes centered at $\mathrm{m}\upsilon_r$, each harmonics corresponds to the beating between a pair of modes separated by m-1 modes in the optical spectrum. At any given value of m, each harmonics will have integer m^2 proportional multiple to the 1st harmonic linewidth, and related to *D* given by [14]

$$\Delta\nu_{RFm} = \Delta\nu_{RF1} m^2 = 2\pi\nu_r{}^2 D m^2 \tag{5}$$

From the coefficients of Eq. (5), the relationship between the first harmonic RF spectrum linewidth and timing jitter diffusion constant *D* can be extracted and are given by

$$\Delta\upsilon_{RF1} = 2\pi\upsilon_r{}^2 D \tag{6}$$

The RF spectrum could be possible perturbed by amplitude noise as with AML laser [8]. Higher harmonics of the photocurrent could be used to distinguish between phase noise and amplitude noise. However, in PML laser, the amplitude noise is dominated by the phase, consequently using any different order of the harmonics has no influence on the RF linewidth [11] as shown in Eq. 5. From Eq. (3) and (6), the optical mode linewidth $\Delta\upsilon_n$ and RF harmonic linewidth $\Delta\upsilon_{RF1}$ are related by way of [13], [14]

$$\Delta\upsilon_n = \Delta\upsilon_{\min} + \Delta\nu_{RF1}(n - n_{\min})^2 \tag{7}$$

Eq. (7) shows that the first harmonic RF linewidth $\Delta\upsilon_{RF1}$ of the semiconductor PML laser can be estimated from measuring the optical linewidth, i.e., optical phase noise, of each longitudinal mode and performing a parabolic fit as a function of mode number. This does not require a direct measurement of the RF PSD which for a high repetition rate laser necessitates

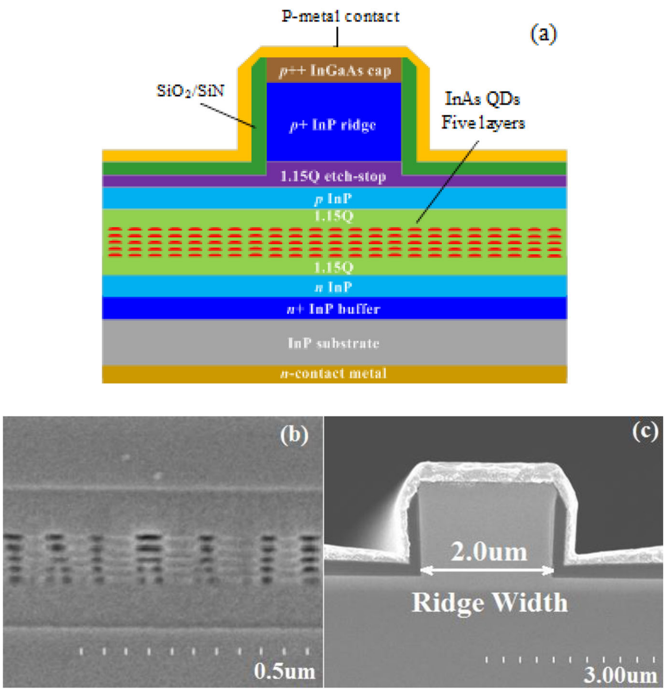

Fig. 1. (a) Schematic cross-sectional diagram of a shallow-etched ridge-waveguide InAs/InP QD CCL; (b) a cross-sectional SEM image of the five-layer InAs/InP QD core region; (c) a cross-sectional SEM image showing the facet of a fabricated FP InAs/InP QD CCL.

the use of a high speed photodetector. Therefore, this method is not restricted to measuring lasers with repetition rates below ~100 GHz. The pulse-to-pulse RMS timing jitter σ_{ptp} can be expressed by the first harmonic RF spectrum linewidth $\Delta\upsilon_{RF1}$ as [11]

$$\sigma_{ptp} = \frac{1}{\upsilon_r}\sqrt{\frac{\Delta\upsilon_{RF1}}{2\pi\upsilon_r}} \tag{8}$$

where $\Delta\upsilon_{RF1}$ can be obtained by parabolic curve fitting the measured optical linewidth as a function of optical mode number as shown in Eq. (7). In the same method, the pulse to clock timing jitter, also called RMS integrated timing jitter could be expressed by $\Delta\upsilon_{RF1}$ as shown in Eq. (18) and (19) in Ref. [14].

III. Materials and Devices

Fig. 1(a) shows a schematic cross-sectional diagram of an etched ridge-waveguide InAs/InP QD coherent comb laser. The InAs/InP QD CCLs were grown by chemical beam epitaxy (CBE) on exactly (100) oriented n-type InP substrates. The QD lasers with repetition frequencies υ_r of 11, 25, 34.5 GHz investigated in this work were fabricated from the same wafer. The laser active region consisted of five stacked layers of InAs quantum dashes embedded in an undoped 350 nm thick InGaAsP (1.15Q) waveguide core as the gain medium. This was surrounded by n- and p- type InP cladding layers and capped with a heavily doped thin InGaAs layer to form a low resistance Ohmic contact. This structure provides both carrier and optical confinement in the QD region. Fig. 1(b) shows a cross-sectional scanning electron microscopy (SEM) image of a five-layer InAs/InP QD

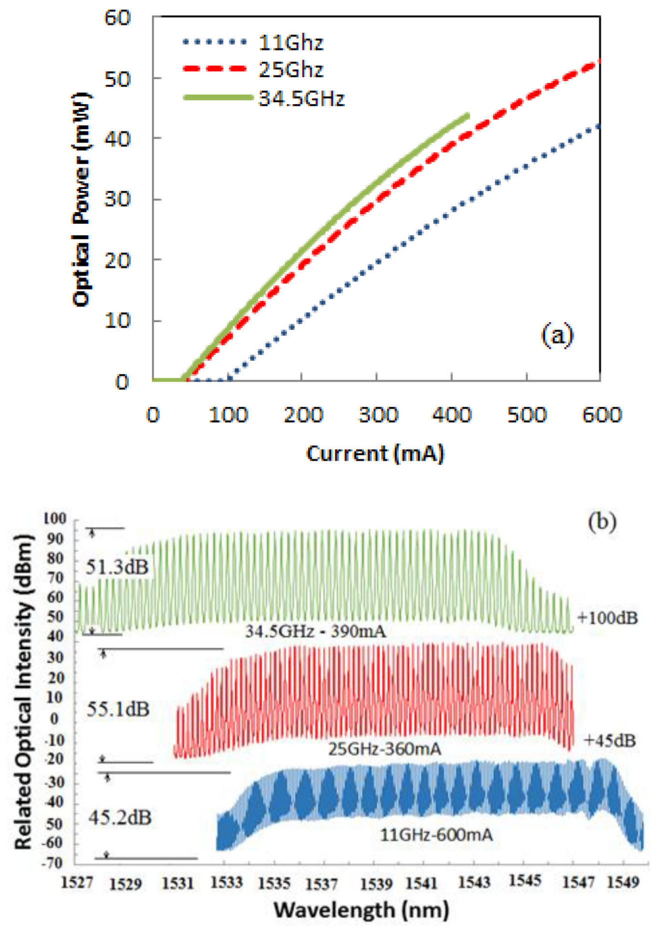

Fig. 2. (a) Light-current characteristics (b) Optical spectra of 11, 25 and 34.5 GHz QD CCL measured by Anritsu MS9740A optical spectrum analyzer at 0.01 nm resolution.

core region. More detailed information of the QD CCL material growth is contained in Ref. [21]. The wafer was fabricated into single lateral mode ridge waveguide lasers with ridge widths of 1.8, 2.0, and 2.6 μm. Devices were then cleaved to form Fabry-Perot laser cavities with cavity lengths of 3848, 1693 and 1225 μm to provide mode spacings of 11, 25 and 34.5 GHz respectively. Fig. 1(c) shows a cross-sectional SEM image of the facet of a fabricated Fabry-Perot laser, no facet coatings were used. The lasers were mounted and wire-bonded onto a chip-on-carrier platform and driven with an ultra-low-noise battery powered laser diode driver. A temperature controlled heat sink was used to maintain an operating temperature range of 16–20 °C. These lasers passively self-mode-lock with a pulse repetition rate corresponding to the F-P mode spacing, i.e., 11, 25 and 34.5 GHz, resulting in well-defined phase correlations between the lasing modes.

IV. Experimental Results and Discussions

Fig. 2(a) shows the light output of the lasers as a function of drive current with blue dots for 11 GHz, red dashes for 25 GHz, and green solid for 34.5 GHz lasers at a heatsink temperature of 20 °C. Fig. 2(b) shows the lasing spectra at the indicated drive

TABLE I
SUMMARY OF STATIC PERFORMANCE OF THE THREE LASERS AT A TEMPERATURE OF 20 °C AND INJECTION CURRENTS OF 600, 360, AND 390 mA FOR THE 11, 25, AND 34.5 GHz DEVICES RESPECTIVELY

	Laser Mode Spacing		
	11 GHz	*25 GHz*	*34.5 GHz*
Threshold (mA)	100	44	39
Differential Efficiency	0.109	0.126	0.14
Resistance (Ω)	1.31	1.46	1.56
Centre Wavelength (nm)	1543.4	1540.7	1537.5
3 dB Spectral Width (nm)	10.2	10.9	12.5
3 dB Number of Modes	116	55	45
10 dB Spectral Width (nm)	14.2	13.4	14.9
10 dB Number of Modes	162	67	54
OSNR (dB)	45.2	55.1	51.3

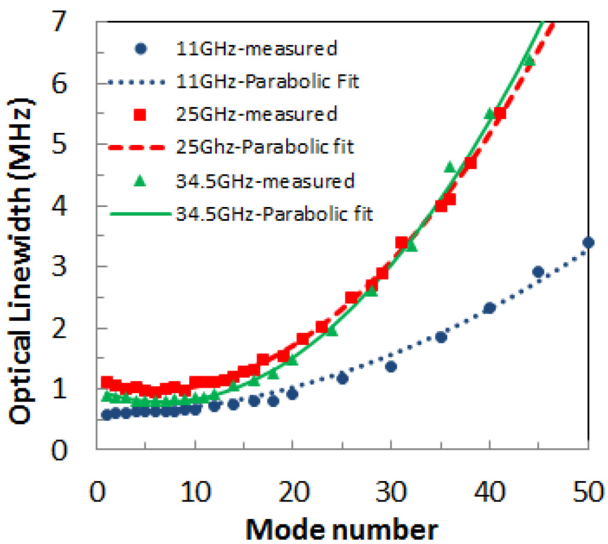

Fig. 3. Measured laser mode optical linewidths vs. mode number and parabolic fits for 11, 25 and 34.5GHz QD CCL by using OEWaves OE4000 automated laser linewidth/phase noise measurement system.

current for the three lasers. The static lasing characteristics are summarized in Table I at injection currents of 600, 360, and 390 mA for the 11, 25, and 34.5 GHz devices respectively. As is typical for Fabry-Perot semiconductor lasers longer cavity reduces the series resistance and lowers the differential efficiency [22]. The central lasing wavelength also increases with increased cavity length due to a corresponding decrease in the total cavity loss as expressed per unit length. This reduces the threshold current density, hence increasing the wavelength of the peak gain at threshold.

Fig. 3 shows the measured optical linewidth for individually filtered longitudinal lasing modes as a function of mode number (dots) for the three lasers. The linewidth is obtained by analyzing the frequency noise spectra using an optical auto-correlator (OE4000 automated laser linewidth/phase noise measurement system, OEWaves Inc.). A Santec OTF-350 optical tunable filter is used for filtering the individual longitudinal lasing modes. The results are average from five measurements. The measured wavelength ranges are from 1548.7 nm to 1538.6 nm (covering 115 modes), 1545.2 nm to 1537.0 nm (covering 41 modes),

TABLE II
RESULTS OF PARABOLIC FIT, USING EQ. (7), OF $\delta \upsilon_{\mathbf{nim}}$, D, N_{nim}, $\delta \upsilon_{\mathbf{RF1}}$ AND STANDARD ERROR OF $\delta \upsilon_{\mathbf{RF1}}$ FROM MEASURED CURVES OF LINEWIDTH VS. OPTICAL MODE NUMBER FOR 11, 25 AND 34.5 GHz QD CCL AND FOR THE SIMILAR LASERS AT 39.6 GHz IN REF. [14]. THE RESULTS OF DIRECT MEASUREMENT OF THE RF LINEWIDTH USING A HIGH SPEED PHOTODETECTOR ARE SHOWN IN THE LAST COLUMN

υ_r GHz	*Fit from Phase noise vs. Mode Number*						*Measured $\Delta\upsilon_{RF1}$*	
	$\Delta\upsilon_{nim}$ MHz	D fs	n_{nim}	$\Delta\upsilon_{RF1}$ kHz	$\Delta\upsilon_{RF1}$ Error kHz	Timing Jitter σ_{ptp} fs	$\Delta\upsilon_{RF1}$ kHz	Timing Jitter σ_{ptp} fs
11	0.59	1.4e-3	0.02	1.07	0.05	11.31	1.09	11.42
25	0.97	9.1e-3	5.6	3.57	0.43	6.03	3.51	5.98
34.5	0.79	0.6e-3	6.6	4.17	0.13	4.02	4.42	4.14
39.6	6.5	9.2e-3	12.0	92	3.0	15.16	89	15.1

and 1541.6 nm to 1530.0 nm (covering 44 modes) for the 11, 25, and 34.5 GHz lasers respectively. For the 11 GHz laser the full range of mode number are not displayed. The minimum measured linewidth is below 1 MHz for all lasers, and is at the long wavelength side of the lasing spectrum for all devices. The linewidth as a function of mode number is well described by the expression shown in Eq. 7, as demonstrated by the excellent parabolic curve fits shown in Fig. 3.

Table II shows the parabolic fit results of $\delta\upsilon_{\rm nim}$, D, n_{nim}, $\delta \upsilon_{\mathbf{RF1}}$ and standard error of $\delta \upsilon_{\mathbf{RF1}}$ from the optical phase noise measurements using Eq. (7). The minimum linewidths $\Delta\upsilon_{\rm min} = 0.59, 0.97, 0.79$ MHz are extracted for the lasers with $\upsilon_r = 11, 25$ and 34.5 GHz, respectively, which would be the linewidth for all the modes if there was no timing jitter. The timing jitter diffusion constant D and the first harmonic RF linewidths $\Delta\upsilon_{RF1}$ are then extracted from the parabolic fit giving D = 0.0014, 0.0091, and 0.0006 fs, $\Delta\upsilon_{RF1} = 1.07$, 3.57, and 4.17 kHz for the $\upsilon_r = 11$, 25 and 34.5 GHz lasers, respectively. The small standard fitting errors of the $\Delta\upsilon_{RF1}$ as shown in Table II indicate good parabolic shapes in the optical mode linewidth v.s. mode number, and verify the Eq. (7). The RF linewidth is found to increase as the laser repetition rate increases. Table II also shows pulse-to-pulse timing jitters, σ_{ptp}, of 11.31, 6.03 and 4.02 fs obtained from phase noise measurements for the 11, 25 and 34.5 GHz lasers, respectively.

In order to verify this technique for calculating $\delta \upsilon_{\mathbf{RF1}}$ we performed a direct measurement of the RF linewidth using a high speed photodetector as shown in Fig. 4. We focused all modes of each laser onto a 45 GHz IR photodetector (New Focus Model-1014) and monitored the electrical output using a 50 GHz PXA signal analyzer (Keysight Technologies Model N9030A). The RF signal analyzer was set to a 100 Hz resolution bandwidth (RBW) and 100 kHz span. Peak frequencies of 11.032, 24.980 and 34.499 GHz were obtained, consistent with the measured mode spacing from the optical spectra. Fig. 4(a) shows the normalized RF spectra and curve fits for each laser, offset for clarity. The Lorentzian line shapes provide good fits for the measured RF PSD curves for all three lasers. The extracted FWHM Lorentzian linewidths, $\Delta\upsilon_{RF1}$, of 1.09, 3.51, and 4.42 kHz are obtained with standard deviations of 0.0097, 0.053, 0.085 kHz. The $\Delta\upsilon_{RF1}$ values obtained from direct RF PSD are

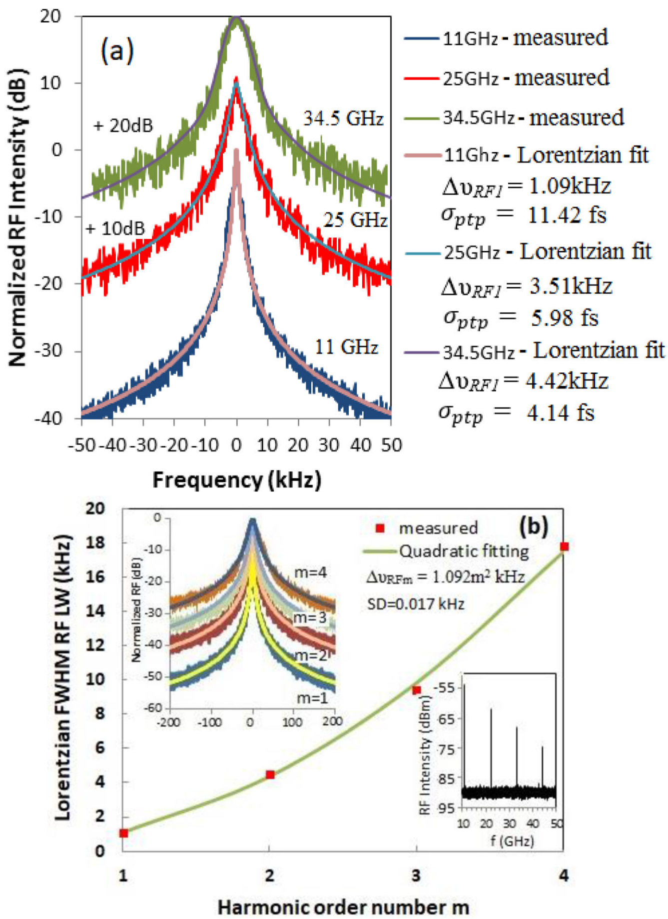

Fig. 4. (a) Normalized first harmonic (m = 1) RF spectra with related Lorentzian fits for 11, 25 and 34.5 GHz QD CCL measured by using Keysight Technologies N9030A 50 GHz PXA signal analyzer at RBW = 100 Hz. (b) Measured RF linewidths as a function of m with Quadratic fit for the laser with $\upsilon_r = 11$ *Ghz*. Inset: upper - RF spectra for m = 1 to 4 and corresponding Lorentzian fits; lower - full span RF spectrum.

very close to those found from the phase noise measurements. The small fitting deviations verify the perfect Lorentzian shape in the RF spectrum and confirmed that $\Delta t(t)$ is in fact a Gaussian random walk process for the PML lasers used in this work. The direct RF linewidth measurement resulted in pulse-to-pulse RMS timing jitters, σ_{ptp}, of 11.42, 5.98, and 4.14 fs for the 11, 25 and 34.5 GHz lasers, respectively. These results are shown in Table II for comparison. The excellent parabolic curve fits of the optical linewidth and the very good agreement between the values of pulse-to-pulse timing jitters obtained from parabolic curve fits of measured optical phase noise with the results from direct RF measurements confirm the validation of the theory of pulse-to-pulse timing jitter from the characterization of optical phase noise for the PML laser. Because of the stochastic process of the timing fluctuations, the timing jitter is actually a statistical average, therefore, there is a certain degree of uncertainty. It is found that the uncertainty in the timing jitter results is not larger than ±20% from the multiple measurements in our experiments.

The linewidths for higher harmonic orders in the RF spectrum have been measured in order to verify Eq. (5) and provides evidence that the amplitude noise is dominated by the phase in the PML laser. Fig. 4(b) shows the fitted Lorentzian linewidths from the measured RF PSD (shown in the upper inset) as a function of harmonic order m with a parabolic fit. The expected quadratic dependence of $\Delta\upsilon_{\rm RFm}$ on m, given by $\Delta\upsilon_{\rm RFm} = 1.097{\rm m}^2$ (kHz), is achieved. The lower inset is a plot of the full span RF spectrum from 10 to 50 GHz with RBW and VBW set at 1MHz and 10 kHz respectively. The 1-4 harmonic peaks are distinctly viewed, however, the peak power of the 4th harmonic is more than 20 dB lower than the 1st harmonic. The small standard deviation 0.0169 of the quadratic fit indicates that the impact of using the 1st harmonic RF linewidth instead a higher harmonic is negligible for our PML laser.

The last row of Table II compares our results with those from Ref [14] which were also obtained from the parabolic fit of the phase noise measurement from a similar QD CCL with $\upsilon_r = 39.6$ GHz. By comparing the overall performance of the device in Ref. [14] to our 34.5 GHz laser we see that the minimum linewidth $\Delta\upsilon_{\min}$ for our device is 8.2 fold lower (0.79 MHz vs. 6.5 MHz); the timing jitter diffusion constant D is 15.3 fold lower (0.0006 fs vs. 0.0092 fs); the RF linewidths $\Delta\upsilon_{RF1}$ is 22 fold lower (4.17 kHz vs. 92 kHz); and the pulse to pulse timing jitter σ_{ptp} is 3.8 fold lower (4.02 fs vs. 15.16 fs). The ultra-low time jitter obtained from the QD PML CCLs studied in this work demonstrates extremely stable mode spacing across the whole comb.

There is a strong connection between the timing jitter of a PML laser and its data bandwidth capability since the timing jitter is strongly related to the optical phase noise of each individual longitudinal mode. Both the modulation data rate and the number N of the higher-order data modulation format, i.e., PAM-N or N-QAM, are inversely proportional to the phase noise of each individual laser channel. If the phase noise or the timing jitter is smaller, we can choose a higher modulation data rate and a larger N to modulate the laser, increasing the data bandwidth.

To demonstrate the performance of these lasers in a high speed data transmission system we test both PAM-4 and QAM-16 modulation schemes. Fig. 5(a) shows the experimental setup for the PAM and QAM data transmission system where the optical modulation is performed by a dual polarization QAM transmitter. A PAM-4 base-band signal is created using the arbitrary waveform generator (AWG) for a NRZ pseudo-random bit sequence with a pattern length of $2^{15}-1$ bits at a symbol rate of 28 GBaud on two uncorrelated channels (*IY and IX*) in the transmitter. Fig. 5(b) shows the Bit Error Rate (BER) as a function of received optical power for B2B and after 25 km of SMF transmission using a single filtered wavelength mode at 1547.855 nm (one of the 48 channels) in the 34.2 GHz laser. The upper inset shows the measured eye diagram at −15dBm received optical power after 25 km SMF transmission showing open eyes. The lower inset shows the measured BER at all 48 channels at −15 dBm received optical power for B2B and after 25-km of SSMF transmission. It is shown that at some channels the performance after 25-km SSMF transmission are better than that of B2B configuration due to the dispersion of fiber would cancel the effect of the chirp induced by the optical modulator [23]. The potential aggregate transmission capacity for the 48

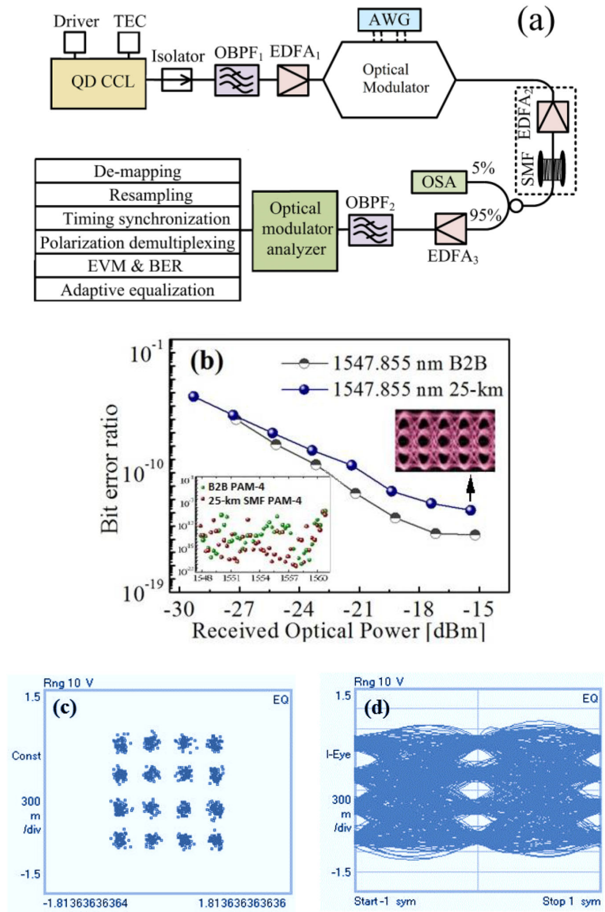

Fig. 5. (a) A schematic of PAM 4 and QAM data format transmission system. (b) Measured BER versus received optical power for PAM 4 B2B and after 25-km of SMF transmission using the comb lines located at 1547.855 nm of 34.2 GHz QD CCL. The inset: upper - eye diagram at selected channel for 25-km of SMF transmission; lower - BER spectrum for B2B and after 25-km of SMF transmission. (c) A constellation (d) eye diagram obtained from filtered channel of 1544.16 nm for the 25 GHz QD CCL in the double polarization 16-QAM data format at 23 GBaud B2B transmission.

channels available using the 34.2 GHz laser is 5.4 Tbit/s (PAM-4 48 $\times$ 28 GBaud PDM) over 25 km of standard single mode fiber transmission. Fig. 5(c) shows a 16-QAM constellation diagram, and 5(d) shows the eye diagram at a symbol rate of 23 GBaud obtained from a filtered single laser mode at 1544.16 nm for the 25 GHz laser with self-injection feedback locking. An error vector magnitude (EVM) of 7.74% and bit-error-rate of 6.15×10^{-6} were obtained. We obtained 16-QAM results at the base rate of 23 GBaud over 56 individual channels, which corresponds to an aggregate transmission capacity of 10.3 Tbit/s (16 QAM 56 $\times$ 23 GBaud PDM) back-to-back (B2B) [2]. The high transmission capacities achieved here verify the low timing jitter for the QD PML laser obtained in this work.

V. Conclusion

We have investigated the pulse-to-pulse time jitter obtained from optical phase noise measurements in 11, 25, and 34.5 GHz C-band InAs/InP QD single-section coherent comb lasers (CCLs). These results are compared to those from a directly measured RF mode beating spectrum. Very good agreement is achieved between the two methods which verified the theory. The method of employing optical phase noise can be used in higher frequency semiconductor passively mode-locked CCLs, which is restricted by the other methods. Pulse-to-pulse time jitter of about 11, 6 and 4 fs is achieved in 11, 25, and 34.5 GHz QD CCLs. By using these lasers, we have successfully demonstrates aggregate data transmission capacities of 5.4 Tbit/s (PAM-4 48 $\times$ 28 GBaud PDM) with over 25-km of standard single mode fiber and 10.3 Tbit/s (16 QAM 56 $\times$ 23 GBaud PDM) with back-to-back (B2B) system.

References

[1] D. Arsenijevi´c, M. Kleinert, and D. Bimberg, “Breakthroughs in photonics 2013: Passive mode-locking of quantum-dot lasers,” *IEEE Photon. J.* vol. 6, no. 2, Apr. 2014, Art. no. 0700306.

[2] Z. Lu, “Quantum-dot coherent comb lasers for terabit optical networking systems,” *Proc. SPIE*, vol. 10921, 109210N-1–109210N-10, Mar. 2019.

[3] P. Bardella, L. L. Columbo, and M. Gioannini, “Self-generation of optical frequency comb in single section quantum dot Fabry–Perot lasers: A theoretical study,” *Opt. Express*, vol. 25, pp. 26234–26252, 2017.

[4] W. W. Chow, S. Liu, Z. Zhang, J. E. Bowers, and M. Sargent III, “Multimode description of self-mode locking in a single-section quantum-dot laser,” *Opt. Express*, vol. 28, pp. 5317–5330, 2020.

[5] F. Lelarge *et al.*, “Recent advances on InAs/InP quantum dash based semiconductor lasers and optical amplifiers operating at 1.55 μm,” *IEEE J. Sel. Top. Quantum Electron.*, vol. 13, no. 1, pp. 111–124, Jan.-Feb. 2007.

[6] K. Merghem *et al.*, “Pulse generation at 346 GHz using a passively mode locked quantum-dash-based laser at 1.55 μm,” *Appl. Phys. Lett.*, vol. 94, no. 2, 2009, Art. no. 021107.

[7] D. J. Derickson, P. A. Morton, J. E. Bowers, and R. L. Thornton, “Comparison of timing jitter in external and mono-lithic cavity mode-locked semiconductor lasers,” *Appl. Phys. Lett.*, vol. 59, no. 26, pp. 3372–3374, Dec. 1991.

[8] D. Von Der Linde, “Characterization of the noise in continuously operating modelocked lasers,” *Appl. Phys. B*, vol. 39, pp. 201–217, 1986.

[9] L. Drzewietzki, S. Breuer, and W. Elsaßer, “Timing jitter reduction of passively mode-locked semiconductor lasers by self- and external-injection: Numerical description and experiments,” *Opt. Express*, vol. 21, no. 13, pp. 16142–16161, 2013.

[10] L. A. Jiang, S. T. Wong, M. E. Grein, E. P. Ippen, and H. A. Haus, “Measuring timing jitter with optical cross correlations,” *IEEE J. Quantum Electron.*, vol. 38, no. 8, pp. 1047–1052, Aug. 2002.

[11] F. Kefelian, S. O’Donoghue, M. T. Todaro, J. G. McInerney, and G. Huyet, “RF linewidth in monolithic passively mode-locked semiconductor laser,” *IEEE Photon. Technol. Lett.*, vol. 20, no. 16, pp. 1405–1407, Aug. 2008.

[12] Y. Takushima, H. Sotobayashi, M. E. Grein, E. P. Ippen, and H. A. Haus, “Linewidth of mode combs of passively and actively mode-locked semiconductor laser diodes,” *Proc. SPIE*, vol. 5595, pp. 213–227, 2004.

[13] T. Habruseva, S. O’Donoghue, N. Rebrova, F. Kéfélian, S. P. Hegarty, and G. Huyet, “Optical linewidth of a passively mode-locked semiconductor laser,” *Opt. Lett.*, vol. 34, no. 21, pp. 3307–3309, 2009.

[14] R. Rosales, K. Merghem, A. Martinez, F. Lelarge, A. Accard, and A. Ramdane, “Timing jitter from the optical spectrum in semiconductor passively mode locked lasers,” *Opt. Express*, vol. 20, no. 8, pp. 9151–9160, 2012.

[15] Z. G. Lu *et al.*, “High performance InAs/InP quantum dot 34.462-GHz C-band coherent comb laser module,” *Opt. Express*, vol. 26, pp. 2160–2167, 2018.

[16] J. R. Liu, Lu Z. G., S. Raymond, J. P. Poole, J. P. Barrios, and D. Poitras, “Dual-wavelength 92.5 GHz self-mode-locked InP-based quantum dot laser,” *Opt. Lett.*, vol. 33, no. 15, pp. 1702–1704, Aug. 2008.

[17] G. Z. Lu, R. J. Liu, J. P. Poole, Y. C. Song, and D. S. Chang, “Ultra-narrow linewidth quantum dot coherent comb lasers with self-injection feedback locking,” *Opt. Express*, vol. 26, no. 9, pp. 11909–11914, Apr. 2018.

[18] Y. Mao, J. Liu, Z. Lu, C. Song, and P. J. Poole, “Ultra-low timing jitter of quantum dash semiconductor comb lasers with self-injection feedback locking,” *IEEE J. Select. Topics QE*, vol. 25, no. 6, Nov. 2019, Art. no. 1900607.

[19] J. P. Tourrenc *et al.*, “Experimental investigation of the timing jitter in self-pulsating quantum-dash lasers operating at 1.55 μm,” *Opt. Express*, vol. 16, no. 22, pp. 17706–17713, 2008.

[20] F. X. Kartner *et al.*, “Few-cycle pulses directly from a laser,” *Top. Appl. Phys.*, pp. 73–136, 2004.

[21] P. J. Poole, K. Kaminska, P. Barrios, Z. G. Lu, and J. R. Liu, “Growth of InAs/InP-based quantum dots for 1.55 μm laser applications,” *J. Cryst. Growth*, vol. 311, no. 6, pp. 1482–1486, 2009.

[22] L. A. Coldren, S. W. Corzine, and M. L. Masanovic, *Diode Lasers and Photonic Integrated Circuits*. NY, USA: Wiley, 2012.

[23] G. Liu *et al.*, “Passively mode-locked quantum dash laser with 5.4 Tbit/s PAM-4 transmission capacity,” *Opt. Express*, vol. 28, no. 4, pp. 4587–4593, 2020, doi: 10.1364/oe.386266.

Youxin Mao received the B.S. degree in physics and the M.S. degree in electronics science from the Nankai University, China, in 1982 and 1985, respectively, and the Ph.D. degree in opto-electronics from Lancaster University, U.K., in 1995. From 1985 to 1992, she was a Lecturer in Electronic Engineer Department, Tianjin University, China. From 1995 to 1997, she was a Research Associate with Lancaster University, and from 1997 to 1999, she was a NSERC Visiting Fellow with the National Research Council in Canada. As a Research Scientist, she worked in Exploratory R&D group with JDS Uniphase from1999 to 2003 and with Medical Biophysics at the University of Toronto from 2003 to 2006. Since 2006, she has been a Senior Research Officer with National Research Council, Canada. She is the author of over 100 peer reviewed articles. Her research interests include quantum dot semiconductor laser, PAM and QAM data format coherent optical network, high speed and high power wavelength swept laser, semiconductor laser package, fiber optics, ultra-small optical fiber probe, and optical coherence tomography.

Zhenguo Lu is a Principal Research Officer, Team Lead of Photonics and Project Leader of National Challenge Program “HTSN” in Advanced Electronics and Photonics Research Centre of National Research Council (NRC), Ottawa, Canada. He also serves as an Adjunct Professor at the Department of Electrical & Computer Engineering of both, University of Ottawa and Concordia University in Canada since 2006. After obtaining his Ph.D. in 1992, he was the recipient of the Alexander von Humboldt (AvH) Research Fellowship for his work at the Institute of Semiconductor Electronics, RWTH Aachen, Germany from 1993 to 1995. Then he worked at Terahertz Research Centre of Rensselaer Polytechnic Institute, NY, USA for two years. Dr. Lu came to NRC as a Research Officer in 1997. From 2000 to 2002, Dr. Lu was the Director of R & D of BTI Systems Inc. He has re-joined NRC as a Senior Research Officer. Dr. Lu is an expert in the field of photonics devices and system applications. He has over 250 publications in the refereed journals and conference papers, and has seven US patents.

Jiaren Liu was born in Sichuan, China in 1963. He received the B.S. and M.S. degrees in physics from the University of Sichuan, Chengdu, China in 1983 and 1989, respectively, and the Ph. D degree in optics from the Nanjing University of Science and Technology in 1992. He was a Teaching Assistant with the Department of Physics, University of Sichuan from 1983 to 1987, an Associate Research Scientist at Shanghai Institute of Optics and Fine Mechanics, Shanghai from 1992 to 1996, a Postdoctoral Research Associate with Texas A&M University, USA and University of Toronto, Canada from 1996 to 1999, and a Product Design Engineer and Manager from 1999 to 2001. Since 2001, he has been a Senior Research Officer with the National Research Council Canada. He is the author of more than 150 peer reviewed articles and several patents. His research interest includes quantum dot semiconductor lasers, fiber lasers, femtosecond laser micromachining, photonic devices, laser spectroscopy, quantum optics, and information optics.

Philip J. Poole received the B.Sc. degree in physics and the Ph.D. degree in solid state physics from Imperial College, University of London, in 1989 and 1993 respectively. Since 1993 he has been working with the National Research Council Canada (NRCC) in the areas of semiconductor optics and crystal growth. He is presently the Team Leader of the Epitaxy Team in the Advanced Electronics and Photonics Research Centre with the NRCC. His work has covered many areas of III-V semiconductor research including optical spectroscopy, quantum well intermixing and 22 years of experience in CBE growth of III-V compounds. His research interests are in the areas of epitaxial growth of InP-based quantum dot structures for optoelectronic devices that can take advantage of the novel properties of quantum dots, such as multiwavelength and femtosecond modelocked lasers. The use of selective area epitaxy to control the nucleation site of individual quantum dots for quantum information purposes is also studied. In particular the growth of InP nanowires containing InAs dots with the demonstration of non-classical optical properties such as photon antibunching and entanglement.

Guocheng Liu received the Ph.D. degree in electrical and computer engineering from the University of Waterloo, Canada, in 2015. From 2016 to 2017, he was a Postdoctoral Fellow at the University of Waterloo. From 2017 to 2019, he worked as an Optical Device Scientist at VueReal Inc. Since 2019, he has been a Research Associate with the National Research Council, Canada. His research mainly focuses on quantum dot semiconductor laser, ultrahigh-speed PAM, and QAM coherent optical networks.